https://doi.org/10.5194/tc-2019-51
Preprint. Discussion started: 13 June 2019

The Cryosphere Discussions

Surface energy fluxes on Chilean glaciers: measurements and models

Marius Schaefer[1], Duilio Fonseca[1], David Farias-Barahona[2], and Gino Casassa[3,4]

[1]Instituto de Ciencias Física y Matemáticas, Facultad de Ciencias, Austral University, Valdivia, Chile
[2]Institute of Geography, Friedrich-Alexander-Universität Erlangen-Nürnberg, Erlangen, Germany
[3]Dirección General de Aguas, Ministerio de Obras Públicas, Santiago, Chile
[4]Universidad de Magallanes, Punta Arenas, Chile

Correspondence: Marius Schaefer (mschaefer@uach.cl)

Abstract. The surface energy fluxes of glaciers determine surface melt and their adequate parameterization is one of the keys for a successful prediction of future glacier mass balance and freshwater discharge. Chile hosts glaciers in a large range of latitudes under contrasting climatic settings: from 18°S in the Atacama Desert to 55°S on Tierra del Fuego Island. We found the Patagonian glaciers to experience higher surface melt rates as compared to the glaciers of the Central Andes due to a higher contribution of the turbulent flux of sensible heat, less negative longwave radiation balance and a positive contribution of the turbulent flux of latent heat. Glaciers in the Central Andes melt at higher rates at cloud-free conditions whilst glaciers in Patagonia melt faster on cloudy days. The models underestimated the measured emissivity of the clearsky atmosphere in the Wet Andes. The different parameterizations of the turbulent fluxes of sensible and latent heat show similar variability but different absolute values due to different parameterizations of the transport coefficients and stability corrections. We conclude that when working towards physical melt models it is not sufficient to use the observed melt as a measure of model performance: the model parameterizations of individual components of the energy balance have to be validated individually against measurements.

1 Introduction

Glaciers are retreating and thinning in nearly all parts of the planet and it is expected that these processes are going to continue under the projections of global warming (Stocker et al., 2013). For mountain glaciers melt is mostly determined by the energy exchange with the atmosphere at its surface. The processes leading to this exchange of energy are complex and depend on the detailed (micro-)climate on the glacier. Classical empirical melt models (like for example degree day models (Braithwaite, 1995)) are getting more and more replaced by more complex models which try to quantify the detailed physical processes that govern the energy exchange at the glacier surface. These kind of models are sometimes called "physical melt models".

https://doi.org/10.5194/tc-2019-51
Preprint. Discussion started: 13 June 2019

Chile is well-known for the climatic variety due to its north-south extension of the territory (4000 km, 17°30 – 55°S), where the Andes range acts as a natural barrier and the Pacific anticyclone plays a key role (Fuenzalida-Ponce, 1971; Garreaud, 2009). Despite the different classifications of sub-glaciological zones (Lliboutry, 1998; Masiokas et al., 2009; Barcaza et al., 2017) most authors agree that there is a transition from Dry Andes to Wet Andes at around 35°S (Figure 1.). The Central Andes of Chile (31°-35°S) are characterized by a Mediterranean climate, with dry conditions during summer. For the period 1979–2006 Falvey and Garreaud (2009) observed a cooling in the coast and a considerable temperature increase of +0.25°C/decade inland in the Maipo River catchment in the Central Andes. Precipitation in this area is highly variable, and predominantly occurs during winter (Falvey and Garreaud, 2007) controlled by El Niño Southern oscillation (ENSO) and the Southeast Pacific Anticyclone (Montecinos and Aceituno, 2003). Between 2010 and 2015 a mega-drought was observed in the Central Andes (Boisier et al., 2016; Garreaud et al., 2017). In the northern part of the Wet Andes (35°-44°S), known in Chile as the Lake District, the elevation range steadily decreases, and wetter climatic conditions are predominant. A general decrease of precipitation in the region was observed during the 20th century (Bown et al., 2007; González-Reyes and Muñoz, 2013). The Southern part of the Wet Andes, Patagonia, is characterized by a hyper-humid climate (Garreaud, 2018), where the largest glacierized areas in the Southern Hemisphere outside Antarctica can be found. This hyper-humid condition has been recently interrupted by a severe drought during 2016 with a precipitation decrease of more than 50% (Garreaud, 2018). Under these different climatic settings, Chile hosts the majority of glaciers in South America (more than 80% of the area), which are mostly thinning and retreating in the last decades (e.g. Braun et al. (2019)). The projections of future changes in climate depend on the different climatological/glaciological zones. This is why a detailed analysis of the processes that determine the energy exchange at the surface of the glaciers in the different climatological zones is necessary, to be able to make reliable predictions of future surface mass balance and melt water discharge of Chilean glaciers.

There exist few surface mass balance observation programs on Chilean glaciers: the only glacier with a climatologically relevant long-term record is Echaurren Norte Glacier near to Santiago de Chile, whose annual surface mass balance is observed since 1975 (WGMS, 2017; Masiokas et al., 2016; Farías-Barahona et al., 2019). Echaurren Norte Glacier (33.5°S) has a general negative trend in its cumulative surface mass balance but also shows stable phases in the 1980s and the first decade of the 21st century, (Masiokas et al., 2016; WGMS, 2017; Farías-Barahona et al., 2019). The variations of the surface mass balance of this glacier can be mostly explained by variations of precipitation in the region (Masiokas et al., 2016; Farías-Barahona et al., 2019). In the semi arid Pascua Lama Region (29°S) several small glaciers have been monitored since 2003 (Rabatel et al., 2011). These glaciers also show mostly negative surface mass balance and are losing area (Rabatel et al., 2011). Here, the limited accumulation of snow is not able to make up with the ablation processes which are dominated by sublimation (MacDonell et al., 2013). In the Chilean Lake District Mocho Glacier is monitored since 2003 (Rivera et al., 2005). Here, a very high inter-annual variability of the surface mass balance was observed (Schaefer et al., 2017). But, on average, the annual surface mass balance was negative which coincides with the observed areal losses (Rivera et al., 2005).

Energy balance studies have been realized in Chile on different glaciers: in the semi-arid Andes MacDonell et al. (2013) quantified in detail the drivers of ablation processes on Guanaco Glacier (29°S). They found that the net shortwave radiation is the main source and that the net longwave radiation and turbulent flux of latent heat are the main sinks of energy at the surface

https://doi.org/10.5194/tc-2019-51
Preprint. Discussion started: 13 June 2019

The Cryosphere
Discussions
Open Access
EGU

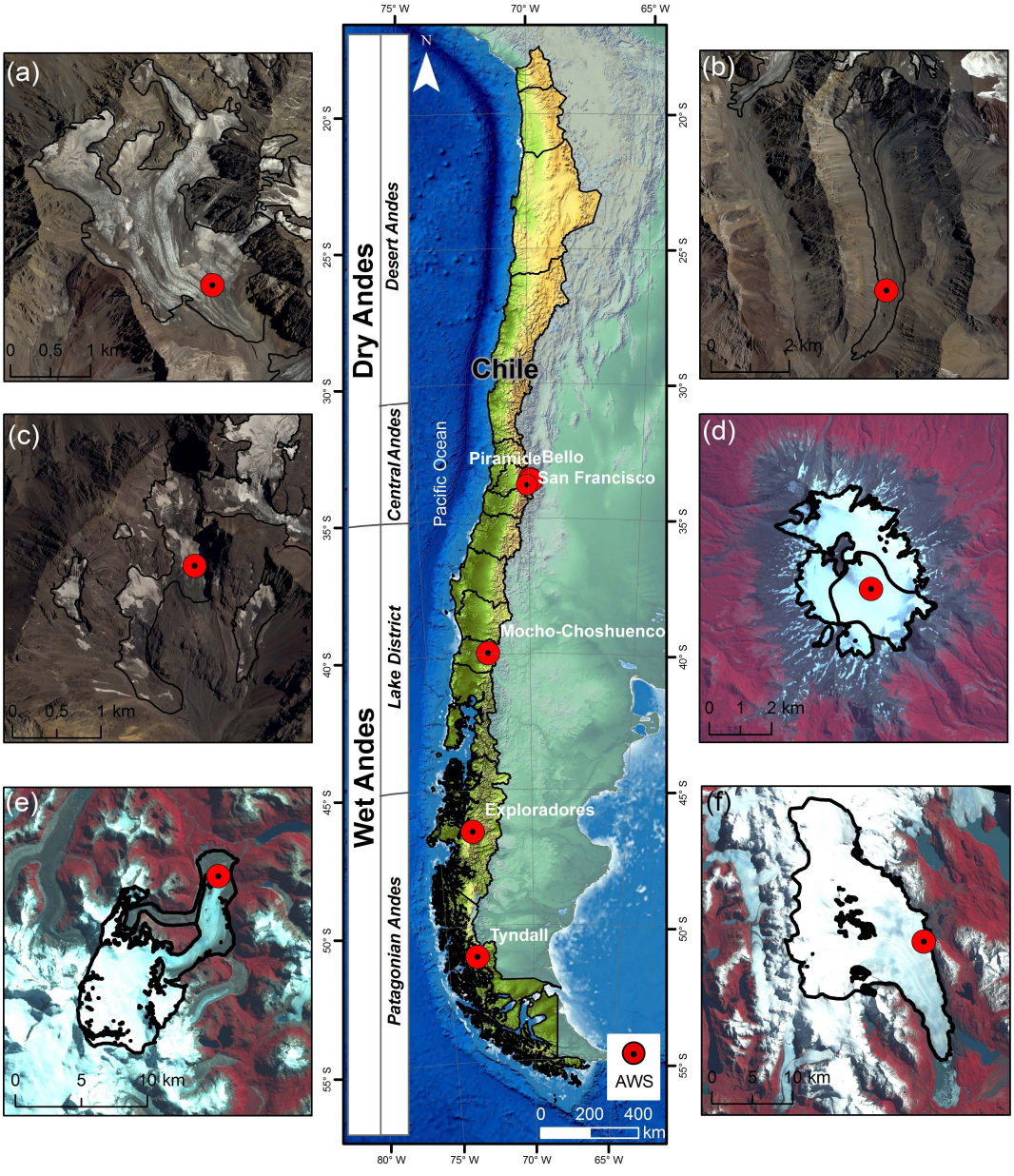

Figure 1. Middle: glaciological zones in Chile according to Lliboutry (1998) and locations of the studied glaciers: (a) Bello Glacier, (b) Pirámide Glacier, (c) San Francisco Glacier, (d) Mocho Glacier, (e) Exploradores Glacier, (f) Tyndall Glacier.

https://doi.org/10.5194/tc-2019-51
Preprint. Discussion started: 13 June 2019

of Guanaco Glacier (MacDonell et al., 2013). Due to the low temperatures on this high elevation site (5324 m a.s.l), they found that sublimation dominated the surface ablation and surface melt contributed only during summer month. Pellicciotti et al. (2008) studied the surface energy balance during summer at Juncal Norte Glacier in the Central Andes (33°S, near Santiago de Chile. Similar to MacDonell et al. (2013) they found that the net shortwave radiation is the main source and that the net longwave radiation and turbulent flux of latent heat are the main sinks of energy. Similar results concerning the influence of the different components of the surface energy balance where obtained by Ayala et al. (2017), who analyzed meteorological data collected on six glaciers in the semiarid Andes of North-Central Chile at elevations spanning from 3127 m.a.s.l. to 5324 m.a.s.l. .

Brock et al. (2007) studied the surface energy balance of bare snow and tephra-covered ice on Pichillancahue-Turbio Glacier (39.5°S) on Villarrica Volcano in the Chilean Lake District during two summers. They found a strong reduction of surface melt on the tephra-covered part of the glacier and a change in sign of the turbulent flux of latent energy to a source due to the higher vapor pressure caused by a more humid atmosphere as compared to the northern and central part of Chile. In southernmost Chile, Schneider et al. (2007) studied the energy balance in the ablation area of Lengua Glacier, which is an outlet Glacier of Gran Campo Nevado Ice Cap (53°S). They found that during February to April 2000, due to the high air temperatures and the high wind speeds turbulent flux of sensible heat was the main source of melt energy for the glacier surface.

In a comparative study of the surface energy balance of glaciers at different latitudes, Sicart et al. (2008) found that the net shortwave radiation is driving the glacier melt at equator near Zongo Glacier, but that at Storglaciären in Northern Sweden the turbulent fluxes of sensibel heat and latent heat dominated the melt patterns.

In this study we analyze meteorological observations that where made on six glaciers distributed in the different glaciological zones of Chile (Figure 1), five of them being equipped and maintained by the Unit of Glaciology and Snows of the Chilean Water Directory (UGN-DGA) (UChile, 2012; Geoestudios, 2013; CEAZA, 2015). Using the meteorological observations as input, we compare different ways to compute the glacier surface energy balance: we use direct measurements of the radiative fluxes at the glacier surface and two models that are freely available: the spreadsheet-based point surface energy balance model (EB-model) developed by Brock and Arnold (2000) and the Coupled Snowpack and Ice surface energy Mass balance model (COSIMA) (Huintjes et al., 2015b, a).

Instead of validating the ability of the energy balance calculations to adequately predict melt rates, in this study we want to test their ability to reproduce the individual energy fluxes: we want to emphasize the differences between the model parameterizations and their ability to reproduce the directly measured radiative fluxes at the glacier surfaces. We also compare three different parameterization for the turbulent fluxes of sensible and latent heat.

2 Sites

In the Central Andes, San Francisco (1.5 km^2) and Bello (4.2 km^2) Glaciers are mountain glaciers which are partially debris-covered at their termini and Pirámide Glacier (4.4 km^2) is a almost completely debris-covered glacier (Figure 1). On the San Francisco and Bello Glacier the AWS were installed over bare ice and at Pirámide Glacier they were installed over debris-

https://doi.org/10.5194/tc-2019-51
Preprint. Discussion started: 13 June 2019

cover. Mocho Glacier is part of the ice cap (14 km^2) which is covering the Mocho-Choshuenco volcanic complex, located in the Lake District (Schaefer et al., 2017). Exploradores Glacier (83.8 km^2) is located on the northern margin of Northern Patagonia Icefield with a prominent portion of debris-cover at its tongue. Finally, Tyndall Glacier (309.8 km^2) is one of the large glaciers in the Southeastern part of the Southern Patagonia Icefield. All glacier areas are from Barcaza et al. (2017).

Due to the installation of new automatic weather stations (AWSs) on several glaciers in the country by the UGN-DGA, detailed meteorological observations from glaciers in the different glaciological zones are available now (UChile, 2012; Geoestudios, 2013; CEAZA, 2015). In Table1 we present the detailed locations of the AWSs used for this study and some relevant glacier parameters.

Table 1. Study period and geographical information of the glaciers and automatic weather stations.

Glacier	**Period**	**Latitude**	**Longitude**	**Elevation**	ELA	Exposure
Name		°	°	m a.s.l.	m a.s.l.	
Bello	01/01/2015-31/03/2015	-33.53	-69.94	4134	4600 (Ayala et al., 2016)	SE
Pirámide	01/01/2016-31/03/2016	-33.59	-69.89	3459	3970 (Ayala et al., 2016)	S
San Francisco	01/01/2016-31/03/2016	-33.75	-70.07	3466	3970 (Carrasco et al., 2008)	SE
Mocho	31/01/2006-21/03/2006	-39.94	-72.02	2003	1990 (Schaefer et al., 2017)	SE
Exploradores	01/01/2015-31/03/2015	-46.51	-73.18	191	1420 (Schaefer et al., 2013)	N
Tyndall	01/01/2015-31/03/2015	-51.13	-73.31	608	1020 (Schaefer et al., 2015)	SE
	01/01/2016-31/03/2016					

Because of its higher relevance for melt modeling, we focused our analysis to summer periods: AWSs of the UGN-DGA have a data record of several years, but during several summers some of the sensors were not working well. In Table 1 we show the selected summer period for every station. For Tyndall Glacier two summers were analyzed. On Mocho Glacier an AWS was installed only during a 50 day period during summer 2006. Figure 2 shows photos from the AWS installed on the glaciers Bello, Exploradores and Tyndall.

3 Methods

In this contribution we want to focus on the six most important energy fluxes which in most cases to a very good approximation sum up to the melt energy available at the glacier surface: the incoming solar radiation (SW_{in}), the reflected solar radiation (SW_{out}), the incoming atmospheric longwave radiation (LW_{in}), the longwave radiation emitted by the glacier surface (LW_{out}) and turbulent fluxes of sensible (SH) and latent heat (LH). We will compare three methods to compute these surface energy fluxes for the selected sites. Before presenting the three methods in detail, we describe the input data for our energy balance calculation in the following section.

https://doi.org/10.5194/tc-2019-51
Preprint. Discussion started: 13 June 2019

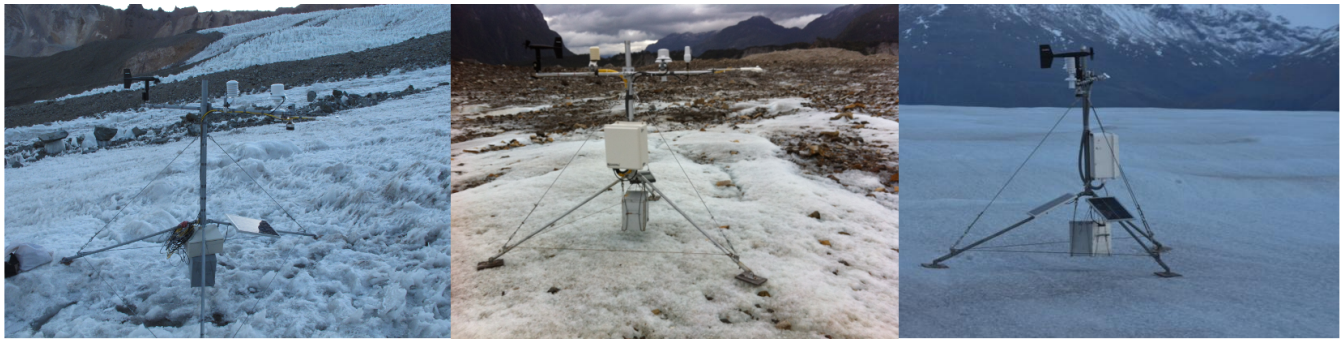

Figure 2. AWS on Bello Glacier (left), Exploradores Glacier (middle) and Tyndall Glacier (right)

3.1 Input data

In Table 2 we present the sensors used at the Mocho-AWS in 2006 and the instruments used at the DGA stations on the other glaciers. The main difference in the installation is the CNR4 sensor, which is installed on the DGA stations and provides detailed measurements of all radiative fluxes, while on Mocho Glacier SW_{in}, SW_{out} and the net allwave radiation is measured. At Mocho-AWS mean values of the data were recorded every 15 minutes, which were resampled to hourly data for the energy balance calculations. At the DGA stations hourly means are recorded and transmitted by a satellite connection. Data at missing hours were interpolated by taking the mean value of the hour before and after the missing one. For Bello Glacier the time resolution of the acquired data changed from hourly to three hourly on 20th of March 2015. Hourly data were generated using a matlab interpolation scheme.

Table 2. Sensors employed at the different AWSs

Variable	AWS-DGA	nominal accuracy	AWS Mocho	nominal accuracy
Incoming solar SW_{in}	Kipp & Zonen CNR 4	7-8% on daily total	Kipp & Zonen SP-Lite	7-8% on daily total
Reflected solar SW_{out}	Kipp & Zonen CNR 4	7-8% on daily total	Kipp & Zonen SP-Lite	7-8% on daily total
Incoming longwave LW_{in}	Kipp & Zonen CNR 4	7-8% on daily total	-	-
Outgoing longwave LW_{out}	Kipp & Zonen CNR 4	7-8% on daily total	-	-
Net all waveAW_{net}	-	-	NR- lite	$\pm$ 3%
Air Temperature T	HMP60	$\pm 0.6^{\circ}C$	HMP45c	$\pm 0.3^{\circ}$C
Relative Humidity RH	HMP60	max 7%	HMP45c	max 3%
Wind Speed U	Young 05103	0.3 m/s o $\pm$ 1%	Young 05103	$\pm$ 0.3 m/s o $\pm$ 1%

https://doi.org/10.5194/tc-2019-51
Preprint. Discussion started: 13 June 2019

3.2 Reference database

We call this first method the reference database, since in this approach direct measurements of the first four fluxes (the radiative fluxes) are used (with the exception of the Mocho-AWS where the net longwave radiative flux is inferred from the incoming solar radiation, the reflected solar radiation and the overall net radiative flux).

The turbulent fluxes of sensible and latent heat were calculated according to two formulas derived in Cuffey and Paterson (2010). The bulk aerodynamic approach is employed and the following important assumptions are made:

- the wind velocity, temperature and water vapor pressure have logarithmic profiles with the same scaling length z_0.
- the shear stress in the first few meters of the atmosphere above the glacier surface is constant.
- the eddy diffusivity for heat has the same value as the eddy diffusivity for water vapor and the eddy viscosity.

Using these assumptions, the following expression for the turbulent flux of sensible heat can be derived:

$$SH = c_a \rho_a C^*(z) U(z) \left[T(z) - T(s)\right], \tag{1}$$

where c_a is the specific heat of air at constant pressure which was assumed to be constant at 1.01 kJ/(kg K) , ρ_a is the air density, $U(z)$ is the wind speed measured at the height z above the surface, $T(z)$ is the air temperature at the height z of the sensor (two meters in our case) and $T(s)$ is the temperature of the glacier-atmosphere interface, which is assumed to be 0°C in this approach.

The dimensionless number $C^*(z)$ is a proportionality constant called the transfer coefficient. In theory it should depend on the measurement height of the sensors of wind velocity and temperature z and the roughness length z_0 according to:

$$C^*(z) = \frac{\kappa^2}{ln^2(z/z_0)}, \tag{2}$$

where κ is the von Karman constant, which has an approximate value of 0.4. In practice however the roughness/scaling length z_0 is variable in space and time (Brock et al., 2006). There exist several recommendations in the literature of values for $C^*(z)$ that have produced satisfying results Cuffey and Paterson (2010), which gives $C^*(z)$ rather the interpretation of a tuning parameter than a physical constant. In our approach we chose a constant roughness length of z_0=0.5 mm, which according to table* 5.4 in Cuffey and Paterson (2010) corresponds to value between smooth ice and ice in the ablation zone and also is inside the range recommended for new and polar snow. According to equation (2) this gives C^*(2 m)=0.0023.

Using the same arguments from above and assuming that the turbulent flux of latent heat is proportional to the difference of the concentration of water vapor at the glacier surface and the air layer above it,Cuffey and Paterson (2010) derive the following expression :

$$LH = 0.622 \rho_a L_v C^* U(z) \left[P_{\text{vap}}(z) - P_{\text{vap}}(s)\right] / P_a. \tag{3}$$

Here, $P_{\text{vap}}(z)$ and $P_{\text{vap}}(s)$ are the water vapor pressure at the elevation z=2 m above the glacier and at its surface, P_a is the air pressure and L_v is the latent heat of vaporization. The water vapor pressure at z=2 m depends on the (measured)

https://doi.org/10.5194/tc-2019-51
Preprint. Discussion started: 13 June 2019

relative humidity and the saturation water vapor pressure $P_{\text{vap,sat}}$ which depends on the air temperature. In Figure 3.(a) we show measurements of the saturation water vapor pressure at different temperatures (Lide, 2004) and the graphs of several parameterizations of the saturation water vapor pressure as a function of the air temperature, found in the literature (Bolton, 1980; Cuffey and Paterson, 2010; Huintjes et al., 2015a). We decided to use the parameterization proposed in Bolton (1980),

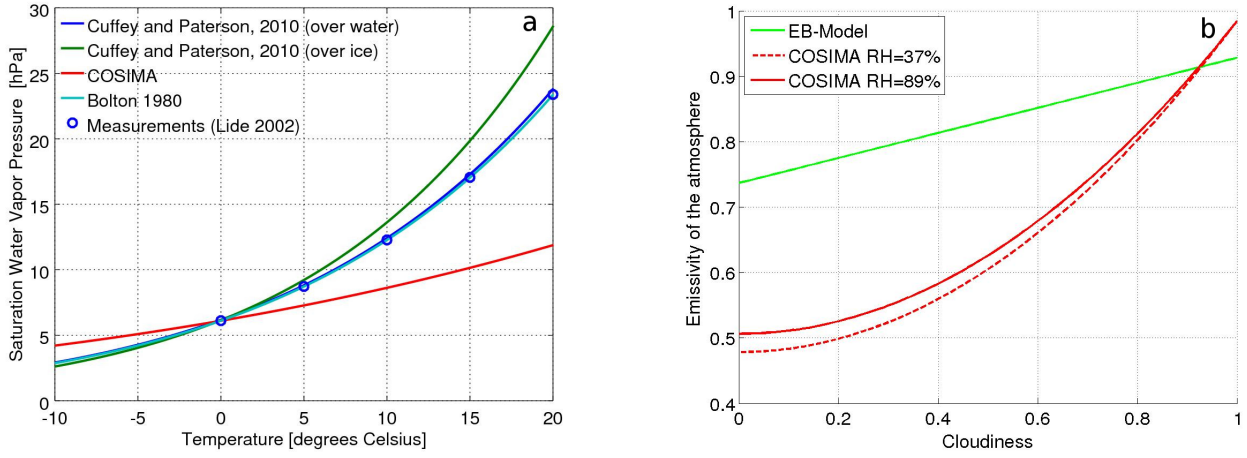

Figure 3. Different parameterizations of the models: (a) saturation vapor pressure as a function of the air temperature, (b) emissivity of the atmosphere as a function of the cloud cover.

since it agrees best with the measurements:

$$P_{\text{vap,sat}}(T) = 6.112 \exp\left(\frac{17.67T}{T+243.5}\right), \tag{4}$$

where $P_{\text{vap,sat}}$ is in hectopascal and the air temperature T is in degrees Celsius. Here it is assumed that at the glacier surface the water vapor pressure is equal to the saturation vapor pressure at 0°C, which is 611 Pascal.

3.3 EB-Model

In the spreadsheet-based energy balance model developed by Brock and Arnold (2000) the incoming solar radiation, two meter air temperature, the wind speed and the water vapor pressure are the meteorological input variables. The fixed input parameters are latitude, longitude and elevation of the station, the aspect and slope, the albedo α and the roughness of the surface z_0. The net shortwave radiation is calculated by multiplying the sum of the direct and diffuse incoming solar radiation by 1-α. The incoming direct and diffuse incoming solar radiation depend on the measured incoming solar radiation SW_{in} and the glacier's surface slope and aspect at the AWS. However, in our study, these parameterizations produced erroneous values for the net shortwave radiation SW_{net} in the late afternoon for several glaciers. This is why we computed SW_{net} from the measured incoming solar radiation SW_{in} by multiplying it with 1-α:

$$SW_{\text{net}} = (1-\alpha)SW_{\text{in}}, \tag{5}$$

https://doi.org/10.5194/tc-2019-51
Preprint. Discussion started: 13 June 2019

where the albedo α is assumed to be a constant, which depends on the characteristics of the glacier surface. This parameterization should exactly agree to the parameterizations proposed in Brock and Arnold (2000) for flat surfaces (zero slope), which should be a very good approximation, since the AWSs are normally placed on flat terrain.

The net longwave radiation is computed by assuming that the snow/ice surface irradiates thermal radiation of a black body at 273.15 Kelvin (0 degrees Celsius) which is 315.6 W/m^2 according to the Stephan-Boltzmann law of thermal radiation. This value is subtracted from the incoming longwave radiation from the atmosphere which is computed with the Stefan-Boltzmann law as well, however this time with an emissivity which is a function of the cloud cover. Brock and Arnold (2000) use a parameterization of the atmospheric emissivity ε which increases linearly as a function of the cloudiness n:

$$\varepsilon_{\text{(EB)}}(n,T) = (1+0.26n)\varepsilon_{\text{cs}}(T), \tag{6}$$

where $\varepsilon_{\text{cs}}(T)$ is the clear sky emissivity which depends on the air temperature T: $\varepsilon_{\text{cs}}(T) = 0.00877T^{0.788}$ (T in Kelvin). The green line in Figure 3 (b) shows the graph of $\varepsilon_{\text{(EB)}}(n,T)$ at five degree Celsius.

The cloudiness is inferred by comparing the theoretically site-specific clear sky incoming solar radiation with the measured incoming solar radiation.

Similar to the reference database, in the EB-Model the turbulent fluxes of latent and sensible heat are calculated by expressions derived from the bulk aerodynamic method (Brock and Arnold, 2000) according to the equations (1) and (3). However, in this model the transport coefficient for the sensible heat flux C^*_{EB1} and latente heat flux C^*_{EB2} have a more complex form and do not only depend on the roughness length z_0 but also on the Monin-Obukhov length scale L and the scaling lengths of temperature z_T and humidity respectively z_H(Brock and Arnold, 2000):

$$C^*_{EB1} = \frac{\kappa^2}{(ln(z/z_0)+5z/L)(ln(z/z_T)+5z/L)} \tag{7}$$

$$C^*_{EB2} = \frac{\kappa^2}{(ln(z/z_0)+5z/L)(ln(z/z_H)+5z/L)} \tag{8}$$

z_H and z_T are calculated as a function of z_0 and the roughness Reynolds number (Brock and Arnold, 2000). Since normally $z_H < z_T < z_0$ (Brock, 2018) and $L > 0$, C^*_{EB1} and C^*_{EB2} are smaller than C^* and $C^*_{EB2} < C^*_{EB1}$.

3.4 COSIMA

The COupled Snow and Ice Melt MAss balance model (COSIMA) was developed at RWTH Aachen (Huintjes et al., 2015b, a) and combines a surface energy balance model with a multi-layer subsurface snow and ice model to compute glacier mass balance (Huintjes et al., 2015a). In this work we want to focus on how COSIMA models the six dominant energy fluxes at the glacier surface. The input parameters for the COSIMA model are the incoming solar radiation (SW_{in}), the two meter air temperature (T), the relative humidity (RH), the wind speed (U), the solid precipitation(P_s), the initial snow height, the air pressure (P) and the cloud cover (n) (Huintjes et al., 2015a). The daily mean cloud cover over the glacier was estimated by comparing the measured SW_{in} with the theoretical, site specific clearsky radiation computed by a code developed by Corripio

https://doi.org/10.5194/tc-2019-51
Preprint. Discussion started: 13 June 2019

(2003). The cloud cover was determined from this cloud transmissivity τ_{cl} by solving the equation proposed in Greuell et al. (1997):

$$\tau_{\text{cl}} = 1 - 0.233n - 0.415n^2. \tag{9}$$

The net solar radiation is calculated using equation 5. In contrast to the EB-Model the albedo is variable and depends on the time since the last snowfall t_{snow} and the thickness h of the snow or firn layer on top of the glacier ice:

$$\alpha = \alpha_{\text{snow}} + (\alpha_{\text{ice}} - \alpha_{\text{snow}}) \exp(-h/d^*), \tag{10}$$

where α_{ice} and d^* are constants and

$$\alpha_{\text{snow}} = \alpha_{\text{firn}} + (\alpha_{\text{frsnow}} - \alpha_{\text{firn}}) \exp(t_{\text{snow}}/t^*), \tag{11}$$

with α_{firn}, α_{frsnow} and t^* being constants as well. This parameterization of snow albedo in COSIMA was tested at Mocho Glacier, where the glacier surface was covered by snow during all the observation period and precipitation data from a near-by automatic weather station were available. On the other glaciers an ice surface and a constant albedo of 0.3 was assumed.

The longwave radiative fluxes are computed using the Stefan-Boltzmann law of thermal radiation as well. The snow/ice surface is considered as a blackbody. However, in contrast to the EB-Model in COSIMA the snow/ice surface temperature is variable depending on the heat fluxes at the glacier-atmosphere interface. Similar to the EB-model the emissivity of the atmosphere is modeled as a function of the cloudiness(n) using the following expression:

$$\varepsilon_{(\text{COS})}(n, T, P_{vap}) = \varepsilon_{cs}(T, P_{vap})(1 - n^2) + 0.984n^2, \tag{12}$$

where the emissivity of the clear sky depends on the air temperature and the water vapor pressure according to the following expression $\varepsilon_{\text{cs}}(T, P_{vap}) = 0.23 + 0.433(P_{vap}/T)^{1/8}$, where T is in kelvin and P_{vap} in pascal. The red graph in Figure 3 (b) shows the variation of $\varepsilon_{(\text{COS})}$ as a function of the cloud cover at five degrees Celsius and assuming different relative humidities.

The turbulent flux of sensible heat in COSIMA $SH_{(\text{COS})}$ is calculated using formula (1). However here SH is multiplied by a correction factor which depends on the bulk Richardson number Ri and which is smaller than one for $Ri > 0.01$ and approaches zero for $Ri = 0.2$ (Huintjes et al., 2015a).

The turbulent flux of latent heat is calculated by the following expression:

$$LH_{(\text{COS})} = 0.622\rho_a L_v C^* U(z) \left[\frac{P_{\text{vap}}(z)}{P_a - P_{\text{vap,sat}}(z)} - \frac{P_{\text{vap}}(s)}{P_a - P_{\text{vap,sat}}(s)} \right]. \tag{13}$$

Since the air pressure P_a is normally much higher than $P_{\text{vap,sat}}$, this formula should give similar results as formula (2). However this expression is multiplied by the same correction factor as SH. Concerning the parameterization of $P_{\text{vap,sat}}$ as a function of temperature, we decided to replace the original parameterization in COSIMA, red line in Figure 3(a), by the parameterization proposed by Bolton (1980), equation (4), since it agrees best with the measurements. The original parameterization of COSIMA underestimates the water vapor pressure at positive temperatures and therefore underestimates LH for positive air temperatures, which are measured during summer at the AWSs (see below).

https://doi.org/10.5194/tc-2019-51
Preprint. Discussion started: 13 June 2019

The Cryosphere Discussions
Open Access
EGU

4 Results

4.1 Glacier climate

In Table 3 we show averages of relevant climatic and glacier surface properties during summer for the six studied glaciers which are ordered according to their latitude from North to South. The mean incoming solar radiation SW_{in} measured on the glacier

Table 3. Mean values of relevant meteorological and glacier surface data during the study periods.

Glacier	SW_{in}	$\alpha_{S\bar{W}_{\text{out}}/S\bar{W}_{\text{in}}}$	$\bar{\alpha}_{\text{daily}}$	LW_{in}	LW_{out}	T	U	RH
	$\left[\frac{W}{m^2}\right]$			$\left[\frac{W}{m^2}\right]$	$\left[\frac{W}{m^2}\right]$	$[C]$	$\left[\frac{m}{s}\right]$	$[\%]$
Bello	297	0.26	0.28	236	306	2.3	2.9	37
Pirámide	282	0.07	0.07	267	362	7.0	4.0	40
San Francisco	211	0.36	0.37	274	318	7.1	2.0	43
Mocho	273	0.57	0.58			5.9	6.3	66
Exploradores	183	0.23	0.24	349	352	7.4	3.1	87
Tyndall 2015	188	0.51	0.52	314	328	4.8	5.6	74
Tyndall 2016	192	0.43	0.45	315	330	5.3	5.7	72

surfaces decreases from North to South due to its latitudinal dependency, due to the higher absorption of the solar radiation in the more humid and cloudy atmosphere in the Wet Andes and due to the fact that the glaciers in Patagonia are located at lower elevations. The AWS on San Francisco Glacier receives considerably less solar radiation than the stations on Bello and Pirámide Glaciers, because of the shade effect from the Mirador del Morado peak in the morning hours (see Figures 1c and A1 in the supplementary material). The mean albedo of the surface was calculated by two methods: firstly by calculating for every day the quotient of the daily sum of outgoing divided by the sum daily incoming solar radiation and taking the average of these values ($\bar{\alpha}_{\text{daily}}$) and secondly by simply dividing the mean outgoing solar radiation by the mean incoming solar radiation over the study period ($\alpha_{S\bar{W}_{\text{out}}/S\bar{W}_{\text{in}}}$). Both methods give similar results. The debris-covered Pirámide Glacier is showing very low albedo. Bello and Exploradores Glacier show low albedo values, which could indicate dirty ice. Tyndall Glacier shows a mean albedo between the literature values of ice and firn. Having a look at the time series of the daily albedo we identified several increases in the albedo, which probably were due to snowfalls. Mocho Glacier is showing a typical mean albedo of firn surfaces. The variation of the albedo during the observation period will be discussed in more detail in the next section. The mean incoming longwave radiation increases from North to South due to the increase in the relative humidity of the atmosphere (see last column), and due to the increased cloudiness in the Wet Andes. The mean outgoing longwave radiation is highest for the debris-covered Pirámide Glacier and lowest for Bello Glacier. The mean air temperature is lowest for the highest station at Bello Glacier and the mean wind velocity is highest for Mocho Glacier.

https://doi.org/10.5194/tc-2019-51
Preprint. Discussion started: 13 June 2019

In order to study the daily cycle of the climatic variables on the glacier we calculated the average value which was measured at every hour of the day during the measurement period which are presented in 4. As expected, the air temperature shows a daily

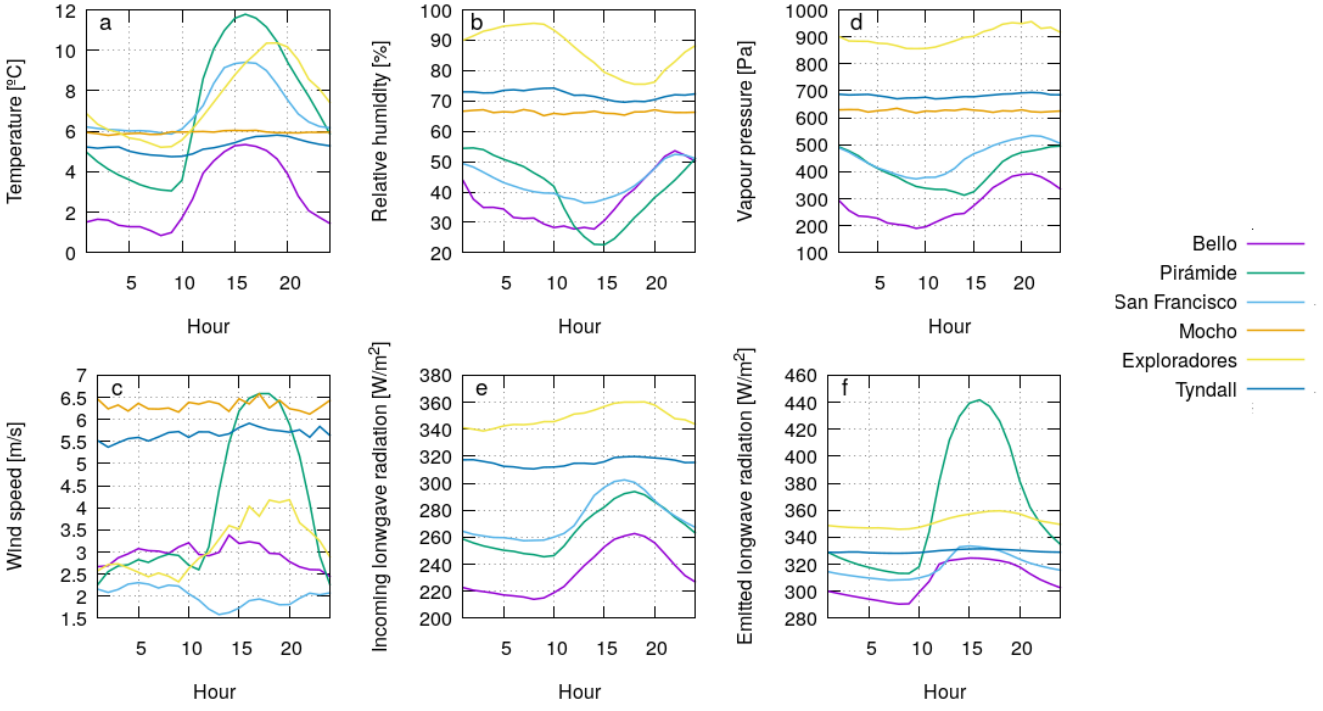

Figure 4. Averages of meteorological variables at the different hours of the day during the study periods on the six studied glaciers: a) temperature T, b) relative humidity RH, c) water vapor pressure P_{vap}, d) wind velocity U, e) incoming longwave radiation LW_{in}, f) outgoing longwave radiation LW_{out}.

cycle for most of the glaciers, with maximum temperatures in the afternoon and minima in the early morning hours. However this daily cycle is much less pronounced for Tyndall Glacier and nearly not present for Mocho Glacier. The relative humidity decreases during the daytime for most of the glaciers. The water vapor pressure shows a maximum during the late afternoon, when the air temperature is still elevated and the humidity is increasing. The wind speed shows a very pronounced increase during the daytime for Pirámide Glacier, when its debris covered surface is heating (Figure 4f). At Exploradores Glaciers an increase in wind speed during the afternoon is observed as well. The incoming longwave radiation show a maximum during the daytime, when the atmospheric temperature is highest. The outgoing longwave radiation, which is emitted by the glacier has a very distinct maximum during the afternoon for Pirámide Glacier (increase of more than 100 W/m^2), which means that the glacier surface is warming during the daytime. Bello, San Francisco and Exploradores Glacier also experience a maximum emission of longwave radiation in the afternoon, whereas Tyndall Glacier shows a constant rate of emission of longwave radiation, which indicates a constant surface temperature during summer.

https://doi.org/10.5194/tc-2019-51
Preprint. Discussion started: 13 June 2019

4.2 Average energy balance and melt

Since two of the applied methods to compute the surface energy balance assume a glacier surface of zero degrees Celsius, we exclude Pirámide Glacier from this analysis. In Figure 5 and Table A1 we present the mean energy fluxes and inferred melt rates for the other five glaciers using the three different methods. In Figure 5 the three columns per glacier correspond

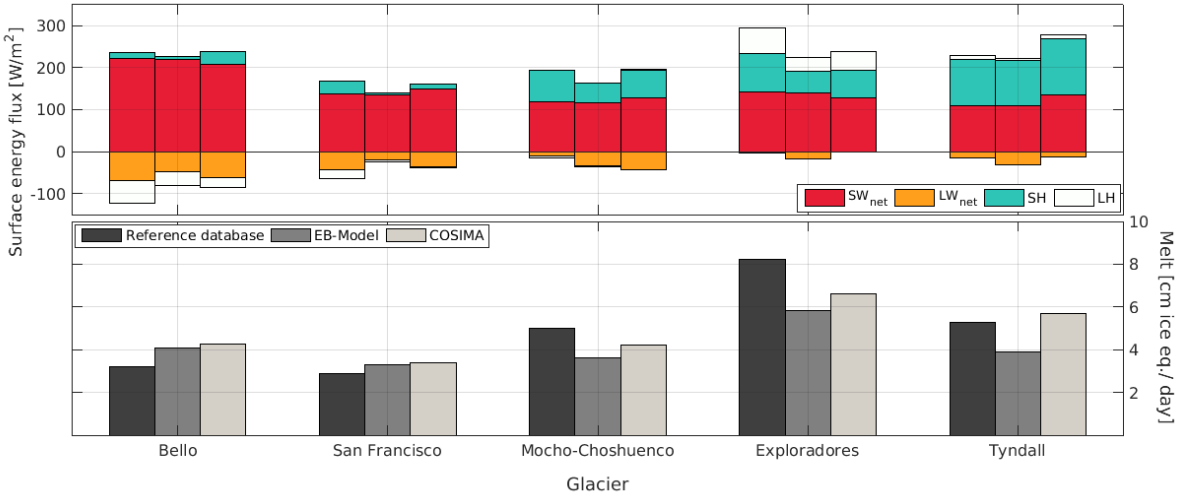

Figure 5. Mean modeled and measured energy fluxes and melt during summer for five glaciers: left bar reference database, middle bar EB-Model, right bar COSIMA.

to reference database, EB-Model and COSIMA from left to right. The net energy flux towards the glacier was converted into daily melt rates in ice equivalent using an ice density of 917 kg/m^3. For Tyndall Glacier in Figure 5 only the results for the summer season 2016 are shown. The mean pattern of the energy fluxes changes from the Central Andes to Patagonia. The net shortwave radiation decreases from North to South. The net longwave radiation is strongly negative in the Central Andes and near to zero in Patagonia. The sensible heat flux is a more important source of energy in Patagonia. The latent energy flux changes sign form sink of energy in the Central Andes to source of energy in Patagonia. This means that in Patagonia water vapor condensates at the surface of the Glaciers, which generates heat for additional melt. There are considerable differences in the prediction of the energy fluxes on the Glacier surfaces between the different methods which will be discussed in detail in the next section. The predicted melt rates are higher for Patagonian Glaciers as compared to the Glacier in the Central Andes.

4.3 Daily energy balance and melt

In this section we analyze how the surface energy fluxes vary from day to day for the different glaciers and what this variations imply for the associated melt rates. In the Figures 6,7,8,12 and 13 we present the computed daily energy fluxes and melt rates for the five studied glaciers. On Bello Glacier the melt rates are clearly modulated by the net shortwave radiation: on days with low net shortwave radiation, days with high cloudiness, the melt rates show clear minima (Figure 6). On Mocho Glacier this

https://doi.org/10.5194/tc-2019-51
Preprint. Discussion started: 13 June 2019

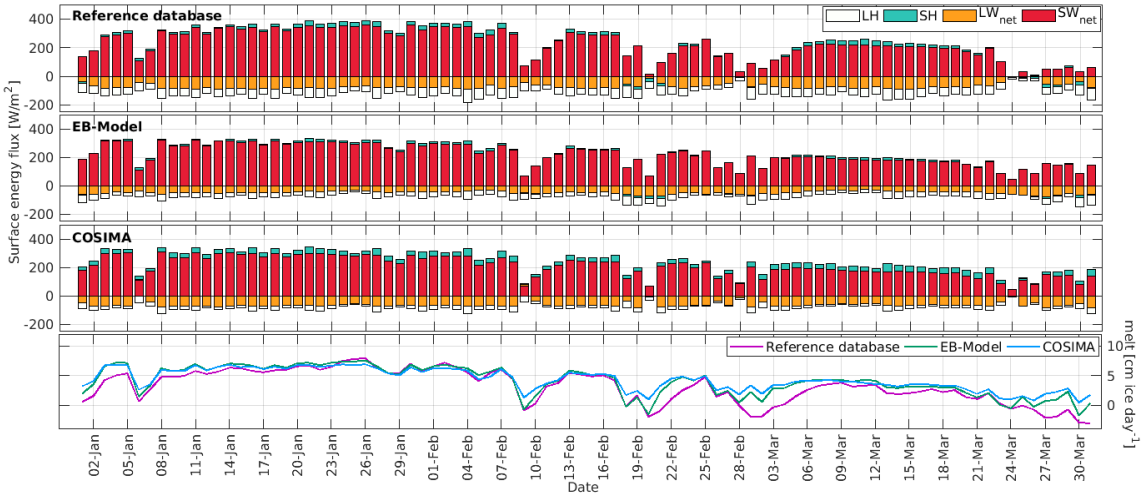

Figure 6. Daily modeled and measured energy fluxes and inferred daily melt rates during summer 2015 for Bello Glacier using the three methods.

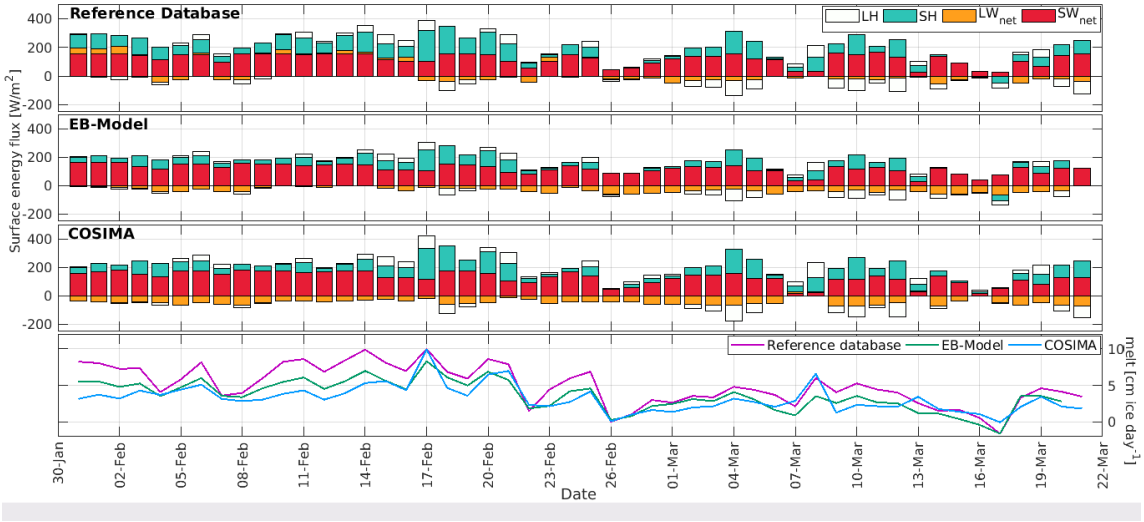

Figure 7. Daily modeled and measured energy fluxes and melt during summer 2006 for Mocho Glacier using the three methods.

https://doi.org/10.5194/tc-2019-51
Preprint. Discussion started: 13 June 2019

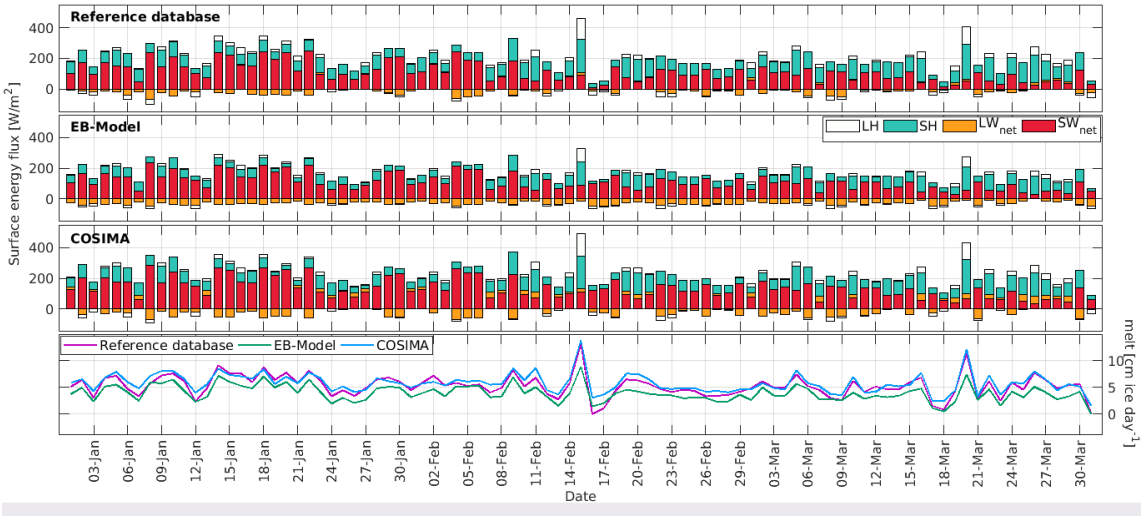

Figure 8. Daily modeled and measured energy fluxes and melt during summer 2016 for Tyndall Glacier using the three methods.

picture changes: high melt rates are rather associated with low net solar radiation, but with high contributions of the sensible heat flux and positive values of the latent heat flux (see for example 17th of February or 18th of March in Figure 7).

Similar results can be observed for Tyndall Glacier: peaks in melt rates are associated to low contribution of the net shortwave radiation and high contributions of the turbulent heat fluxes (15th of February or 20th of March in Figure 8).

5 Discussion

5.1 Glacier climate

The systematic variation of several meteorological variables between the different parts of the Chilean Andes crucially determine the importance of the different energy exchange process at the glacier surfaces (Table 3). The SW_{in} differs around 100 W/m^2 between the Bello and Pirámide Glacier in the Central Andes and Exploradores and Tyndall Glacier in the Patagonian Andes. The difference in SW_{in} between the two glaciers in the Patagonian Andes is only 9 W/m^2, although they have opposite exposition and the difference between one summer and another on Tyndall Glacier is only 4 W/m^2. Another very clear trend form north to south is found for the relative humidity. The values measured in the Patagonian Andes double the values obtained for the central Andes. This influences the latent fluxes: in the Central Andes moisture is transported away from the glacier surfaces whilst in Patagonia moisture is transported towards the glacier surfaces. The higher relative humidity in the Patagonian Andes favors cloud formation, which explains the higher LW_{in} for the Patagonian Andes. The mean values for LW_{out} detected on the glaciers are surprisingly higher than the expected 315.6 W/m^2 for a black body at zero degrees Celsius. However considering the instrument's calibration uncertainty of 8%, indicated by the manufacturer, the expected value is within the uncertainty range of the sensor for Bello, San Francisco and Tyndall Glacier. The higher emission of longwave radi-

https://doi.org/10.5194/tc-2019-51
Preprint. Discussion started: 13 June 2019

ation from Pirámide Glacier can be explained by the heating of its debris cover. In the photograph of the AWS at Exploradores Glacier (Figure 2, right image), we can recognize some stones that could be in the field of view of the CNR sensor. The heating of these stones and the very humid and temperate air column between the sensor and the glacier are probably the reason for the elevated LW_{out} value registered at Exploradores Glacier.

Considering the variability of the data from the two summers measured on Tyndall Glacier, we can state that the glacier climate was similar in both summers. Especially mean LW_{in},LW_{out}, RH and U were nearly identical. SW_{in} and T were both a bit lower in 2015 as compared to 2016 and the surface albedo was higher in 2015. The mean values of T,RH and U measured on Tyndall Glacier during the summers 2015 and 2016 were also very similar to the mean values measured by Takeuchi et al. during December 1993 (Takeuchi et al., 1999).

5.2 Parametrizations of the surface energy fluxes

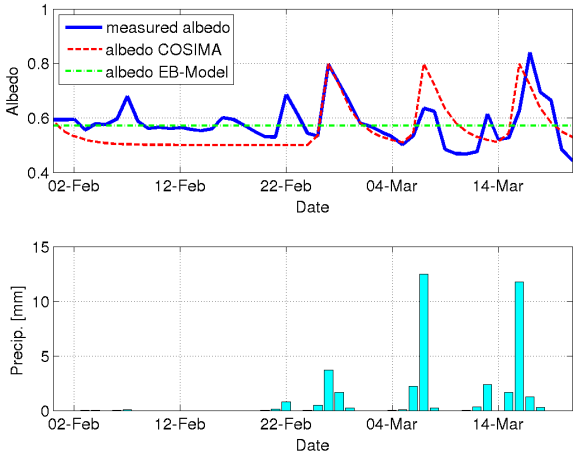

Figure 9. Measured and modeled daily albedo on Mocho Glacier and precipitation registered in Puerto Fuy during summer 2006. The albedo value used in EB-Model corresponds to the mean value of the measured albedo. In COSIMA the following parameters have been chosen: α_{frsnow}= 0.8, α_{firn}= 0.5, time constant t^*= 2 days, snow depth constant d^*= 8 cm (see equations (11) and (12)

The net shortwave radiation is an important source of energy for all the glaciers. According to equation (3) it is determined by the incoming shortwave radiation and the albedo of the surface. Albedo of snow and ice surfaces are very variable and depend on grain size and form, liquid water content, impurities and other factors (Wiscombe and Warren, 1980; Warren and Wiscombe, 1980; Cuffey and Paterson, 2010). Generally fresh snow has the highest albedo which is decreasing in time when snow grains are growing and the snow is eventually getting dirty. COSIMA tries to reproduce this albedo aging effect introducing a snow albedo which exponentially decreases in time (equation 12). In Figure 9 we show the comparison between the measured daily albedo on Mocho Glacier during February and March 2006 and the predictions of the COSIMA model.

https://doi.org/10.5194/tc-2019-51
Preprint. Discussion started: 13 June 2019

It is clearly visible that increases in the albedo are associated with precipitation events registered at the nearby automatic weather station in Puerto Fuy. COSIMA is mostly able to capture these increases. However, in the measured increases in the surface albedo are much more variable than in the one obtained from the model. A drawback of this comparison is certainly that we do not know the exact amount of snow falling on the glacier, but deduce it from the liquid precipitation measured at a automatic weather station in the valley.

The longwave radiative fluxes make important contributions to the energy exchange at the glacier surface. Since snow and ice emit like blackbodies ($\varepsilon = 1$) and the atmosphere mostly shows emissivity smaller than one, the longwave radiation balance is often negative (even at positive ambient temperatures). However in the humid Patagonia the measured net longwave radiation is often balanced (Figure 5 upper panel left bar glaciers Mocho, Exploradores and Tyndall). In Figure 10 we plot the "measured" daily emissivity calculated by inverting the Stefan-Boltzmann law

$$\varepsilon_{\text{measured}} = \frac{LW_{\text{in}}}{\sigma T^4}, \tag{14}$$

where σ denotes the Stefan–Boltzmann constant, as a function of the daily cloudiness. For a direct comparison, we show the parametrizations of the models in the same plot. Generally we can note that the data of the "measured" emissivity shows

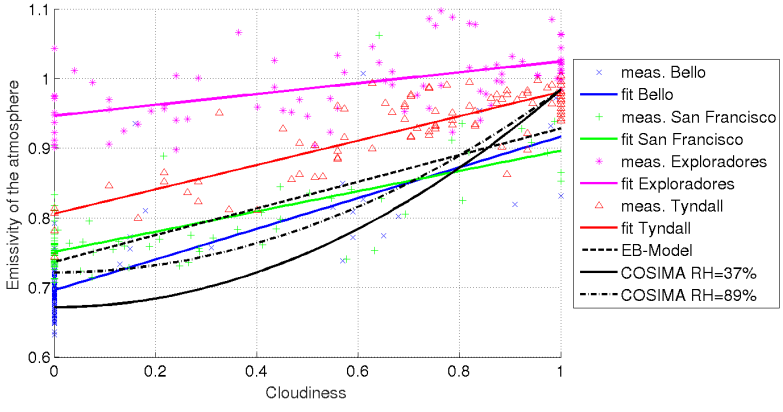

Figure 10. "Measured" emissivity of the atmosphere as a function of the cloudiness. The data points correspond to the daily emissivity obtained from equation (16) by using daily means of LW_{in} and T plotted against the inferred daily cloudiness values using different symbols and colors for every glacier. The straight continuous colored straight lines correspond to linear fits to the data of every glacier and the black line correspond to the model parametrizations.

considerable scatter around their linear trend line. At Exploradores Glacier the measured emissivity reaches values higher than one.

The big scatter of the measured data can be explained by the uncertainties that are associated with the determination of the cloud cover and the emissivity of the atmosphere. The cloud cover data were obtained from the cloud transmisivity of the atmosphere. However there are different parameterization for that available in the literature (see for example Oerlemans (2001)). Also the "measured" emissivity is associated to some uncertainty: it is not clear if the temperature measured at two

https://doi.org/10.5194/tc-2019-51
Preprint. Discussion started: 13 June 2019

meters over the glacier surface is representative for the temperature of the atmosphere which is emitting longwave radiation towards the glacier surface. The emissivity values >1 obtained for Exploradores Glacier, could indicate that the CNR4 is overestimating LW_{in}, which would be in accordance with the elevated values for LW_{out} discussed in section 5.1 . We can recognize that the model parameterizations underestimate the emissivity of the atmosphere over Patagonian Glaciers, especially for low cloudiness conditions. This underestimation of the emissivity of the atmosphere leads to an underestimation of the net longwave radiative balance on clear days for the Patagonian Glacier, which can be recognized in Figures 7,8 and 13.

The variability of the modeled turbulent fluxes is very similar in all three methods. This is expected since the formula to compute these fluxes (1,2,4,5) have very similar aspect: in all approaches the sensible heat flux is mainly driven by the temperature difference of the glacier surface and the atmosphere at two meters elevations and wind speed (equations 1,4) and the latent heat flux is driven by the difference of the water vapor pressure at the glacier surface and the atmosphere at two meters elevations and wind speed (equations 2,5). The absolute values of the turbulent fluxes computed in EB-Model (equations 4,5) are lower than the absolute values computed for the reference database (equations 1,2)(Table 4). This is because the transport coefficients C^*_{EB1} and C^*_{EB2} take lower values than C^*, due to the extra term in the denominator. The sensible heat fluxes modeled by COSIMA are higher in between the ones obtained in the reference database and Eb-Model. Only at Bello Glacier the sensible heat flux modeled by COSIMA is the highest of the three approaches, which can be explained by the modelled cooling of the glacier surface in the night times, which is increasing the temperature difference of the glacier surface and the atmosphere as compared to the other approaches. The turbulent fluxes of sensible heat modeled by COSIMA are mostly slightly more positive, than the ones modelled bt the other two approaches.

5.3 Melt rates

Melt rates ranging from 2.9 to 4.2 cm/day of ice equivalent (cm i.e./day) for the Dry Andes and from 3.6 to 8.2 cm i.e./day for the Wet Andes were predicted by the different approaches of quantifying energy fluxes on the surface of five glaciers (Table 4). These values lie within the range of observed melt range during summer on these glaciers or glaciers with similar climatic conditions.

In the Wet Andes on Mocho Glacier Schaefer et al. (2017) measured ablation rates of 2.6 cm i.e./day and 3.2 cm i.e./day in the summers 2010 and 2011 and measured and inferred rates of 3.6 cm i.e./day and 3.7 cm i.e./day in the summers 2012 and 2013 at the same location where the AWS was installed in 2006. This indicates that the value of 5.0 cm i.e./day inferred by the first method is probably overestimating the melt at this location and that the other two methods are predicting more realistic melt rates. Here, we have to take into account that net longwave radiation was inferred by subtracting the net shortwave fluxes from the net overall radiation, measured with the NR-lite, which is a lower precision instrument as compared to the newer sensors installed in the CR4. At Tyndall Glacier in the period November 2012 to May 2013 an average ablation rate of 3.8 cm i.e./day was observed at two stakes near to the location of the AWS. Considering that this period also includes spring and autumn months, were melt rates should be lower, this in in very good agreement to the values of 3.3 to 5.7 cm i.e./day predicted by the different approaches presented in this work. From January 2015 to March 2015 an average ablation rate of 9.1 cm i.e./day was measured at a stake network installed on Grey Glacier at an elevation range ranging from 260 m.a.s.l. to 380 m.a.s.l.. This

https://doi.org/10.5194/tc-2019-51
Preprint. Discussion started: 13 June 2019

indicates that the 8.2 cm i.e./day predicted by the first approach for Exploradores Glacier seems to be a realistic magnitude for a low elevation site on a glacier in the Patagonian Andes.

In the Dry Andes ablation was measured at a stake network on Bello Glacier during summers 2013/2014 and 2014/2015 (CEAZA, 2015). A high variability of ablation rates in space and time were obtained. Several of the ablation rates inferred for stakes nearby the AWS were of similar size than the predicted ones by the methods presented in this paper. Analyzing the signal of an ultrasonic sensor installed on an ablation gate next to the AWS of San Francisco Glacier we found a surface lowering of 4.9 cm/day during December 2015. Assuming that snow melt in this period of the year with a density of 500 kg/m^3 this yields a rate of 2.7 cm i.e./day, which is in good agreement with the melt rates inferred in this contribution.

5.4 Implications for glaciological zones in Chile

Our results suggest a transition of energy sources for surface melt from the Central Andes to Patagonia. The energy sources obtained for Mocho Glacier at 40°S are more similar to ones observed at the Patagonian glaciers than to the ones observed for the glaciers of the Central Andes, where SW_{in} is the dominating source of energy for melt (Figure 5). The greater importance of the turbulent flux of sensible heat as energy source available to produce surface melt at Mocho Glacier probably contributes to the observed strong dependency of its annual mass balance on the annual mean temperatures measured on a nunatak of the glacier(Scheiter, 2016; Schaefer et al., 2017). This picture changes strongly in the Central Andes, where a very low dependency of the annual mass balance of Echaurren Norte Glacier on the annual mean temperature observed at Embalse el Yeso was reported (Masiokas et al., 2016; Carrasco, 2018; Farías-Barahona et al., 2019). When comparing the importance of the energy sources between the two summers modeled for Tyndall Glacier (Table 4) , we can state that in 2015 SW_{net} was slightly lower than in 2016 due to the lower SW_{in} and the higer surface albedo observed in that year (Table 3). However the overall pattern of energy sources (and sinks) is very similar for both years. All these results confirm the general division of the Chilean Andes into Dry Andes and Wet Andes, with the zonification limit being located approximately at 35°S (Lliboutry, 1998).

5.5 Implications for physical melt modeling and transferability of parametrizations

The capacity of the models to reproduce the measured radiative fluxes is still improvable. The albedo aging effect implemented in COSIMA is a big improvement regarding to constant albedo parameterizations for snow, firn and ice surfaces. However the parameters of this aging formula seem to vary strongly from one site to another and a good calibration of this formula seems to be necessary. Regarding the predictions of the net longwave radiative fluxes on the glacier surface, the parameterization of the emissivity of the atmosphere is crucial. The parameterizations of the tested models both fail to predict the observed incoming longwave radiation on cloud-free days in the humid climate of the Patagonian glaciers (Figure 10). This is because the used parameterizations are fits to data that were obtained in different climatic conditions. Therefore, these parameterizations are not physical and can not be simply transferred to other sites where the conditions are different.

Different parameterizations for the turbulent fluxes of sensible and latent heat were compared in this study, where different parameterizations for the exchange coefficient and possible corrections to it were applied. There are many parameters involved in these parameterizations so that choosing these parameters in a way that the contribution of the turbulent fluxes helps to obtain

https://doi.org/10.5194/tc-2019-51
Preprint. Discussion started: 13 June 2019

the desired (observed) melt rates, seems to be a straight forward task. However, this exercise does not make these formula better predictors in other situations and on other glacier surfaces. Direct measurements of the turbulent fluxes is necessary and the eddy-covariance technique seem to be a promising technique (Cullen et al., 2007).

We think that there is still a strong need to measure the energy exchange processes on the glacier surfaces and we think that coordinated efforts of governmental agencies, such as the Glaciology and Snows Unit of the Chilean Water Directory in our case, can improve our knowledge substantially. If we want to talk about physical melt models, then we have to show the capacity of these models to reproduce the different physical processes that take place at glacier surface. Bringing the predicted melt rates by these highly parameterized models in agreement with the observed ones seems to be rather a curve adjustment exercise than a indicator of correct physics.

6 Conclusions

Performing an extended study of surface energy fluxes during summer on five Chilean glaciers on a north-south transect and under strongly varying climate settings we reached to the following conclusions:

- The contribution of the different energy fluxes between atmosphere and glacier change from the Central Andes towards the Patagonian Andes: the net shortwave radiation as main source of energy at the glacier surfaces in the Central Andes looses importance further South, where the turbulent fluxes of sensible and latent heat are an important source of energy. The net longwave radiation changes from a strong sink of energy for the glaciers of the Central Andes to a net zero contribution in the Patagonian Andes.
- The inferred melt rates were higher for the Patagonian Andes than for the Central Andes.
- Mocho Glacier in the Chilean Lake District is showing similar patterns of surface energy fluxes to the glaciers in the Patagonian Andes.
- The models underestimated the measured emissivity of the clearsky atmosphere in the Wet Andes.
- From our study it is difficult to infer which parameterization of the turbulent fluxes is the most appropriate one. More detailed studies on this topic are necessary, which include direct measurements of these fluxes.
- To develop or improve physical models we have to validate every single model parameterization against data and cannot judge the model's performance only by comparing the final output, since in this highly parameterized models the effect of physically wrong parametrizations might cancel out and the final result might be satisfying, without reproducing well the individual physical processes.
- Openly shared codes are the best way to improve physical models, since everyone can test the individual parameterizations against his data and adjust or improve them accordingly. This is the preferred way to obtain physical parameterizations as opposed to large chains of models which supposedly model physical processes whose individual performance, however, is not validated and the final results rather come out of a black box.

https://doi.org/10.5194/tc-2019-51
Preprint. Discussion started: 13 June 2019

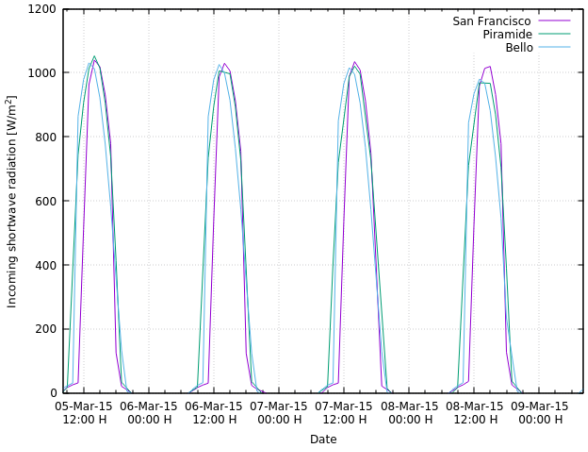

Figure A1. Incoming shortwave radiation at the AWSs installed on Bello, Pirámide and San Francisco Glacier during March 2016.

Author contributions. M.S. designed the research, ran the COSIMA model, wrote the manuscript and prepared several figures, D.Fonseca prepared the reference database, ran EB-Model and prepared several figures, D.Farías provided detailed information about the DGA-AWS and prepared Figure 1, G.C. measured the surface energy fluxes on Mocho Glacier. All authors discussed the results and commented on the manuscript.

Competing interests. no competing interests are present

Acknowledgements. We thank the Chilean Water Directory (DGA) for providing meteorological information and photographs from the automatic weather stations according to "Ley de transparencia solicitud Numbers 76796,76800,76802"

https://doi.org/10.5194/tc-2019-51
Preprint. Discussion started: 13 June 2019

The Cryosphere Discussions
Open Access
EGU

Table A1. Mean values of the computed surface energy fluxes and melt rates during the study periods on the five studied glaciers using the three different methods.

Glacier	Method	SW_{net}	LW_{net}	SH	LH	Melt
		$[\frac{W}{m^2}]$	$[\frac{W}{m^2}]$	$[\frac{W}{m^2}]$	$[\frac{W}{m^2}]$	[cm ice eq./day]
Bello	Reference Database	223	-70	13	-53	3.2
	EB-Model	220	-48	6	-33	4.1
	COSIMA	208	-62	30	-23	4.3
San Francisco	Reference Database	137	-44	30	-21	2.9
	EB-Model	135	-19	6	-5	3.3
	COSIMA	149	-37	12	-2	3.4
Mocho	Reference Database	118	-11	75	-5	5.0
	EB-Model	117	-33	46	-2	3.6
	COSIMA	127	-44	68	2	4.2
Exploradores	Reference Database	143	-3	91	61	8.2
	EB-Model	141	-18	51	32	5.8
	COSIMA	129	-1	64	46	6.6
Tyndall 2015	Reference Database	94	-15	76	8	4.6
	EB-Model	92	-30	52	5	3.3
	COSIMA	132	-13	70	9	5.5
Tyndall 2016	Reference Database	110	-14	83	8	5.3
	EB-Model	109	-29	55	5	3.9
	COSIMA	135	-13	75	8	5.7

References

Ayala, A., Pellicciotti, F., MacDonell, S., McPhee, J., Vivero, S., Campos, C., and Egli, P.: Modelling the hydrological response of debris-free and debris- covered glaciers to present climatic conditions in the semiarid Andes of central Chile, Hydrological Processes, 2016.

Ayala, A., Pellicciotti, F., MacDonell, S., McPhee, J., and Burlando, P.: Patterns of glacier ablation across North-Central Chile: Identifying the limits of empirical melt models under sublimation-favorable conditions, Water Resources Research, 53, 5601–5625, https://doi.org/10.1002/2016WR020126, 2017.

Barcaza, G., Nussbaumer, S. U., Tapia, G., Valdés, J., García, J.-L., Videla, Y., Albornoz, A., and Arias, V.: Glacier inventory and recent glacier variations in the Andes of Chile, South America, Annals of Glaciology, 58, 166–180, 2017.

Boisier, J. P., Rondanelli, R., Garreaud, R. D., and Muñoz, F.: Anthropogenic and natural contributions to the Southeast Pacific precipitation decline and recent megadrought in central Chile, Geophysical Research Letters, 43, 413–421, 2016.

Bolton, D.: The Computation of Equivalent Potential Temperature, Monthly Weather Review, 1980.

https://doi.org/10.5194/tc-2019-51
Preprint. Discussion started: 13 June 2019

Bown, F., Rivera, A., Acuña, C., and Casassa, G.: Recent glacier mass balance calculations at Volcán Mocho-Choshuenco (40°S), Chilean Lake District, in: Glacier Mass Balance Changes and Meltwater Discharge, edited by Ginot, P. and Sicart, J., vol. 318, pp. 143–152, IAHS, Wallingford, Oxfordshire, 2007.

Braithwaite, R. J.: Positive degree-day factors for ablation on the Greenland ice sheet studied by energy-balance modelling, Journal of Glaciology, 41, 153–160, 1995.

Braun, M. H., Malz, P., Sommer, C., Farías-Barahona, D., Sauter, T., Casassa, G., Soruco, A., Skvarca, P., and Seehaus, T. C.: Constraining glacier elevation and mass changes in South America, Nature Climate Change, 9, 130, 2019.

Brock: Personal Comunication., 2018.

Brock, B., Rivera, A., Casassa, G., Bown, F., and Acuna, C.: The surface energy balance of an active ice-covered volcano: Villarrica Volcano, Southern Chile, in: Annals of Glaciology, VOL 45, 2007, edited by Clarke, G. and Smellie, J., vol. 45 of *Annals of Glaciology-Series*, pp. 104–114, https://doi.org/10.3189/172756407782282372, international Symposium on Earth and Planetary Ice-Volcano Interactions, Univ Iceland, Inst Earth Sci, Reykjavik, ICELAND, JUN 19-23, 2006, 2007.

Brock, B. W. and Arnold, N. S.: Spreadsheet-Based (Microsoft Excel) Point Surface Energy Balance Model for Glacier and Snow Melt Studies, Earth Surface Processes and Landforms, 25, 649–658, https://www.researchgate.net/profile/Ben_Brock/publication/229662187_A_spreadsheetbased_(Microsoft_Excel)_point_surface_energy_balance_model_for_glacier_and_snow_melt_studies/links/54abe4aa0cf2ce2df6691cc7.pdf, 2000.

Brock, B. W., Willis, I. C., and Sharp, M. J.: Measurement and parameterization of aerodynamic roughness length variations at Haut Glacier d'Arolla, Switzerland, Journal of Glaciology, 52, 281–297, 2006.

Carrasco, J. F., Osorio, R., and Casassa, G.: Secular trend of the equilibrium-line altitude on the western side of the southern Andes, derived from radiosonde and surface observations, Journal of Glaciology, 54, 538–550, https://doi.org/10.3189/002214308785837002, 2008.

Carrasco, P.: Condiciones hidroclimáticas en los Andes de Santiago, y su influencia en el balance de masa del glaciar Echaurren Norte, Master's thesis, Universidad Austral de Chile, 2018.

CEAZA: Modelación del balance de masa y descarga de agua en glaciares del Norte Chico y Chile Central, Tech. rep., Dirección General de Aguas, S.I.T. No. 382, 2015.

Corripio, J.: Vectorial algebra algorithms for calculating terrain parameters from DEMs and solar radiation modelling in mountainous terrain, International Journal of Geographical Information Science, 17, 1–23, https://doi.org/10.1080/713811744, 2003.

Cuffey, K. and Paterson, W.: The Physics of Glaciers, Elsevier, forth edition edn., 2010.

Cullen, N. J., Mölg, T., Kaser, G., Steffen, K., and Hardy, D. R.: Energy-balance model validation on the top of Kilimanjaro, Tanzania, using eddy covariance data, Annals of Glaciology, 46, 227–233, 2007.

Falvey, M. and Garreaud, R.: Wintertime precipitation episodes in central Chile: Associated meteorological conditions and orographic influences, JOURNAL OF HYDROMETEOROLOGY, 8, 171–193, https://doi.org/10.1175/JHM562.1, 2007.

Falvey, M. and Garreaud, R. D.: Regional cooling in a warming world: Recent temperature trends in the southeast Pacific and along the west coast of subtropical South America (1979-2006), Journal of Geophysical Research, 114, D04 102, https://doi.org/10.1029/2008JD010519, 2009.

Farías-Barahona, D., Vivero, S., Casassa, G., Schaefer, M., Burger, F., Seehaus, T., Iribarren-Anacona, P., Escobar, F., and Braun, M. H.: Geodetic Mass Balances and Area Changes of Echaurren Norte Glacier (Central Andes, Chile) between 1955 and 2015, Remote Sensing, 11, 260, 2019.

Fuenzalida-Ponce, H.: Climatología de Chile, Tech. rep., Departamento de Geofísica, Universidad de Chile, 1971.

https://doi.org/10.5194/tc-2019-51
Preprint. Discussion started: 13 June 2019

Garreaud, R.: The Andes climate and weather, Advances in Geosciences, 22, 3–11, 2009.

Garreaud, R.: Record-breaking climate anomalies lead to severe drought and environmental disruption in western Patagonia in 2016, Climate Research, 74, 217–229, 2018.

Garreaud, R. D., Alvarez-Garreton, C., Barichivich, J., Boisier, J. P., Christie, D., Galleguillos, M., LeQuesne, C., McPhee, J., and Zambrano-Bigiarini, M.: The 2010-2015 megadrought in central Chile: impacts on regional hydroclimate and vegetation., Hydrology & Earth System Sciences, 21, 2017.

Geoestudios: Implementación Nivel 2 Estrategia Nacional de Glaciares: Mediciones Glaciológicas Terrestres en Chile Central, Zona Sur y Patagonia, Tech. rep., Dirección General de Aguas, S.I.T. No. 327, 2013.

González-Reyes, A. and Muñoz, A.: Cambios en la precipitación de la ciudad de Valdivia (Chile) durante los últimos 150 años, BOSQUE, 34, 191–200, 2013.

Greuell, W., Knapp, W. H., and Smeets, P. C.: Elevational changes in meteorological variables along a midlatitude glacier during summer, Journal of Geophysical Research, 102, 25 941–25 954, 1997.

Huintjes, E., Sauter, T., and Schneider, C.: Manual to COSIMA COupled Snowpack and Ice surface energy and MAss balance MODEL, Tech. rep., RWTH Aachen, 2015a.

Huintjes, E., Sauter, T., Schroeter, B., Maussion, F., Yang, W., Kropacek, J., Buchroithner, M., Scherer, D., Kang, S., and Schneider, C.: Evaluation of a Coupled Snow and Energy Balance Model for Zhadang Glacier, Tibetan Plateau, Using Glaciological Measurements and Time-Lapse Photography, Arctic, Antarctic, and Alpine Research, 2015b.

Lide, D. R., ed.: CRC Handbook of Chemistry and Physics, CRC Press, 2004.

Lliboutry, L.: Glaciers of South America, US Geological Survey Professional Paper, 1998.

MacDonell, S., Kinnard, C., Mölg, T., Nicholson, L., and Abermann, J.: Meteorological drivers of ablation processes on a cold glacier in the semi-arid Andes of Chile, The Cryosphere, 7, 1513, 2013.

Masiokas, M. H., Rivera, A., Espizua, L. E., Villalba, R., Delgado, S., and Carlos Aravena, J.: Glacier fluctuations in extratropical South America during the past 1000 years, Palaeogeography Palaeoclimatology Palaeoecology, 281, 242–268, https://doi.org/10.1016/j.palaeo.2009.08.006, 2009.

Masiokas, M. H., Christie, D. A., Le Quesne, C., Pitte, P., Ruiz, L., Villalba, R., Luckman, B. H., Berthier, E., Nussbaumer, S. U., González-Reyes, A., McPhee, J., and Barcaza, G.: Reconstructing the annual mass balance of the Echaurren Norte glacier (Central Andes, 33.5° S) using local and regional hydroclimatic data, The Cryosphere, 10, 927–940, https://doi.org/10.5194/tc-10-927-2016, https://www.the-cryosphere.net/10/927/2016/, 2016.

Montecinos, A. and Aceituno, P.: Seasonality of the ENSO-related rainfall variability in central Chile and associated circulation anomalies, Journal of Climate, 16, 281–296, 2003.

Oerlemans, J.: Glaciers and Climate Change, A.A. Balkema Publishers,Lisse, Abingdon, Exton, Tokyo, 2001.

Pellicciotti, F., Helbing, J., Rivera, A., Favier, V., Corripio, J., Araos, J., Sicart, J.-E., and Carenzo, M.: A study of the energy balance and melt regime on Juncal Norte Glacier, semi-arid Andes of central Chile, using melt models of different complexity, HYDROLOGICAL PROCESSES, 22, 3980–3997, https://doi.org/10.1002/hyp.7085, workshop on Glaciers in Watershed and Global Hydrology, Obergurgl, AUSTRIA, AUG 27-31, 2007, 2008.

Rabatel, A., Castebrunet, H., Favier, V., Nicholson, L., and Kinnard, C.: Glacier changes in the Pascua-Lama region, Chilean Andes (29° S): recent mass balance and 50 yr surface area variations, The Cryosphere, 5, 1029–1041, 2011.

https://doi.org/10.5194/tc-2019-51
Preprint. Discussion started: 13 June 2019

Rivera, A., Bown, F., Casassa, G., Acuna, C., and Clavero, J.: Glacier shrinkage and negative mass balance in the Chilean Lake District (40 degrees S), Hydrological Sciences Journal, 50, 963–974, https://doi.org/10.1623/hysj.2005.50.6.963, 2005.

Schaefer, M., Machguth, H., Falvey, M., and Casassa, G.: Modeling past and future surface mass balance of the Northern Patagonian Icefield, Journal of Geophysical Research Earth Surface, 118, 571–588, https://doi.org/10.1002/jgrf.20038, 2013.

Schaefer, M., Machguth, H., Falvey, M., Casassa, G., and Rignot, E.: Quantifying mass balance processes on the Southern Patagonia Icefield, The Cryosphere, 9, 25–35, 2015.

Schaefer, M., Rodriguez, J., Scheiter, M., and Casassa, G.: Climate and surface mass balance of Mocho Glacier, Chilean Lake District, 40°S, Journal of Glaciology, 63, 218–228, https://doi.org/10.1017/jog.2016.129, 2017.

Scheiter, M.: Mass Balance Modeling on Mocho Glacier, Tech. rep., Universidad Austral de Chile, 2016.

Schneider, C., Kilian, R., and Glaser, M.: Energy balance in the ablation zone during the summer season at the Gran Campo Nevado Ice Cap in the Southern Andes, Global and Planetary Change, 59, 175 – 188, https://doi.org/http://dx.doi.org/10.1016/j.gloplacha.2006.11.033, http://www.sciencedirect.com/science/article/pii/S092181810600292X, mass Balance of Andean Glaciers, 2007.

Sicart, J. E., Hock, R., and Six, D.: Glacier melt, air temperature, and energy balance in different climates: The Bolivian Tropics, the French Alps, and northern Sweden, Journal of Geophysical Research: Atmospheres, 113, 2008.

Stocker, T., Qin, D., Plattner, G.-K., Tignor, M., Allen, S., J. Boschung, A. N., Xia, Y., Bex, V., and Midgley, P., eds.: Summary for Policymakers. In: Climate Change 2013: The Physical Science Basis. Contribution of Working Group I to the Fifth Assessment Report of the Intergovernmental Panel on Climate Change, Cambridge University Press, 2013.

Takeuchi, Y., Naruse, R., Satow, K., and Ishikawa, N.: Comparison of heat balance characteristics at five glaciers in the Southern Hemisphere, Global and Planetary Change, 22, 201–208, 1999.

UChile: Modelación de balance de masa y descarga de agua en glaciares de Chile Central, Tech. rep., Dirección General de Aguas, S.I.T. No. 307, 2012.

Warren, S. G. and Wiscombe, W. J.: A model for the spectral albedo of snow. II: Snow containing atmospheric aerosols, Journal of the Atmospheric Sciences, 37, 2734–2745, 1980.

WGMS: Global Glacier Change Bulletin No. 2 (2014–2015), Tech. rep., U(WDS)/IUGG(IACS)/UNEP/UNESCO/WMO, zemp, M., Nussbaumer, S. U., Gärtner-Roer, I., Huber, J., Machguth, H., Paul, F. and Hoelzle, M. (eds.), 2017.

Wiscombe, W. J. and Warren, S. G.: A model for the spectral albedo of snow. I: Pure snow, Journal of the Atmospheric Sciences, 37, 2712–2733, 1980.